NTNU

**Norwegian University of
Science and Technology**

Modeling and Control of Wave Energy Converters

Marthe Kristine Tautra Hoen

Problem Description

The purpose of the thesis is to investigate different methods for optimal control of buoy-based wave energy converters. This includes mathematical modeling and control of the wave energy converter.

The following elements must be considered:

1. Literature study on wave energy converters. Give a presentation of different methods found in the literature. Identify the main problems from a control point of view, construction as well as implementation aspects. Define the control objective.
2. Derive a mathematical model for a buoy-based wave energy converter. For simplicity, it can be assumed that the wave loads are harmonic.
3. Design and tune a control system for maximum wave energy absorption. Simulate the system in the time-domain and present results for tracking capabilities and energy/power absorption. The system must be simulated for varying wave loads (amplitude and frequency). A mathematical stability analysis of the closed loop system must be included. The system should also be analyzed in presence of forces oscillations using classical techniques.
4. Present your findings and theoretical results in the report.

Assignment given: 17. September 2008
Supervisor: Thor Inge Fossen, ITK

Abstract

Wave Power is a technology that was founded in the 70's, but which still not has reached full industrial recognition as a energy source.

In this thesis there is a literature study on different concepts of Wave Energy Converters(WEC) which has been build in full scale, and there is a great variety in the concepts. There is a theory chapter where ocean waves theory, mass-spring-damper dynamics, hydrodynamics and maximum power capture are presented.

The modeling work was done on a axisymmetric point absorber WEC, which can be said to have the greatest potential for energy absorption because it is small relative to the wavelength of the incident waves.

To be able to simulate on the model, a control strategy must be included, and I have included PID control and Model Predictive Control as strategies to be able to capture maximum power with Phase Latching. I believe that Model Predictive Control will be the best choice for control system, although it is not as robust as PID control, but because of its predictive behavior.

At last there is a chapter where further work and some concluding remarks are given.

Preface

This Master's thesis is the concluding work on my degree in Master of Technologies at Norwegian University of Science and Technology NTNU, Department of Engineering Cybernetics.

I would like to thank my supervisor prof. Thor I. Fossen, who guided me on the right track when I asked for a thesis were I could write about a environmentally friendly technology which could be a part of a sustainable development. His views and ideas in the starting phase of my thesis was of great value for the development of my assignment. He has also been very accessible when I needed some help to move on.

A thank to my co-supervisor Jørgen Hals, PhD Student at Centre of Ships and Ocean Structures is also appropriate. He wrote the paper which is the fundament of this thesis' modeling chapter, and he let me use his model and findings as I wanted.

I have had the honored to write about Ocean Wave Power, a field where outstanding research has been done by people here at NTNU. It has been extra inspiring to have correspondence with one of the most influent man on Wave Power Conversion, prof. Johannes Falnes, who also let me use figures from his textbook "Ocean Waves and Oscillating System".

I would to thank my live-in partner Jarle Steira who has put up with me these months without complaining. He has also given me confident in my work and helpful remarks on my writing. At last, I wouldn't have made this without back up from my parents, thank you!

Trondheim April 1, 2009

Marthe Kristine Tautra Hoen

Contents

List of Figures

List of Tables

Chapter 1

Introduction

1.1   A short history of wave energy makers

The oil crisis in the early 70's made a demand for new energy sources, and so the research on wave energy converters(WEC) started. The researchers recognized the potential the WEC was as energy sources. The Norwegian scientists Kjell Budal and Johannes Falnes from the Norwegian University of Science and Technology NTNU (former University of Trondheim) was two of the pioneers in the research on wave energy makers. They started their cooperation in 1973 by bringing up new ideas on the area (Budal and Falnes 1985), and some of the ideas where later made into theories and physical experiments. At the same time, at the University of Edinburgh, scientist Stephen Salter began his first experiments on different types of heaving floats(Cruz 2007).

1.2   The point absorber wave energy converter

One of the WEC types is the point absorber, and it is the type of scope in this thesis. Usually axisymmetric about a vertical axis, *the point absorber* type of energy converter is an appealling one because is it small relative to the wavelenght of the incident waves as seen in figure 1.1, and therefore the scattering wave field can be neglected and the forces on the body are only due to the incident wave. The potential capture width is large as the point absorbers are capable to absorb the energy from a wavefront many times the key horizontal dimension of the absorber. The point absorbers are of *second generation* among the WECs and they are designed to operate at a wide variety of offshore and nearshore sites where a high level of energy is available.
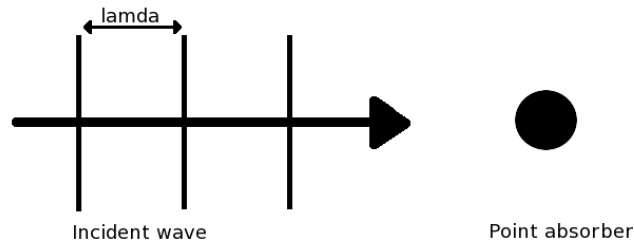
Figure 1.1: Schematic showing scale and orientation of a *Point absorber*

1.3 Full scale wave energy converters

Several concepts for wave energy converters(WEC) have reached the full-scale stage. The four main technologies are as followed(Cruz 2007, ch. 7): The Archimedes Wave Swing, the Oscillating Water Column, the Wave Dragon and the Pelamis. These are investigated in the following subsections.

1.3.1 Archimedes Wave Swing (AWS)

Uniquely among the concepts of WECs, the *Archimedes wave swing* is fully submerged. This is an advantage in case of storms and also because of its non-visibility over water. Shown in figure 1.2(a), the AWS is characterized as a point absorber type, as its diameter is small compared to wavelength. The AWS consists of an air filled chamber fixed to the sea bed. The chamber, called the silo, is open on top. Surrounding the silo is an upside-down cylindrical cup, called the floater. An air lock between the silo and the floater prevents water to get in to silo. The heaving motion of the floater is created due the pressure rise and fall when wave crest directly above the device. The oscillations can be converted into electrical power by the terms of a permanent/magnet linear generator.

1.3.2 Oscillating Water Columns (OWC)

The *Oscillating water columns* are formed by a chamber which is filled with air above the water line as shown in figure 1.2(b). The water level inside the chamber rises and falls due to wave action, alternatly pressurising and rarefying the air within the chamber. Pressurized air escapes from the chamber through a turbine-generator unit producing electrical power. Secondly, when the water level falls, the air is sucked back into the chamber through the turbine-generator assembly to continue power production. The turbine-generator most often used is the Wells turbine. There are also submergded

(a) The Archimedes Wave Swing

(U.S. Department of Energy n.d.)
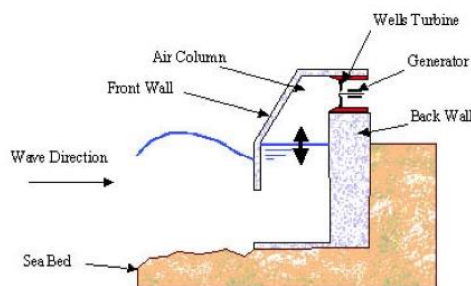
(b) The Oscillating Water Column

(Renewable Energy Journal 2007)

Figure 1.2: The Archimedes Wave Swing and the Oscillating Water Column

OWCs where the chamber is on the seabed.

1.3.3 Wave Dragon

Unlike the other concepts of wave energy conversion, the wave dragon does not oscillate with the waves; it gathers wave energy passively by utilising the overtopping principle. The drawing in figure 1.3 illustrates the overtopping principles and how the captured water is drained through the turbines. The front face of the device is formed as a curved ramp. There are long reflector wings mounted to the reservoir whose purpose are to channel the waves to the ramp where the waves surge upon, as if it was a beach. Behind the crest of this ramp there is a reservoir where the overtopping water with higher potential energy than the surrounding water is gathered. The extraction of energy happens when the water drains back to the sea through low head hydro turbines within the reservoir. The wave dragon has dimensions of 300 metres wide and 170 metres deep, and is made of concrete. This means that it will be very stable, and therefore less vulnerable to fatigue problems.

1.3.4 The Pelamis

Figure 1.4 shows the *Pelamis*, which is a semi-submerged, articulate-structured wave energy converter composed by cylindrical sections linked by hinged joints. The Pelamis is held on station by a compliant mooring system that allows the machine to weathervane to align itself head-on to incoming waves. When waves travel along the body, the Pelamis perform an snake-like motion
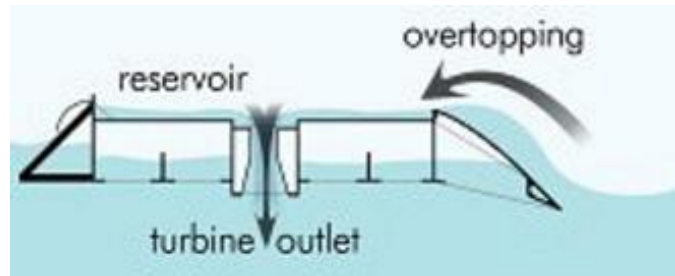
Figure 1.3: The Wave Dragon
(Wave Dragon n.d.)
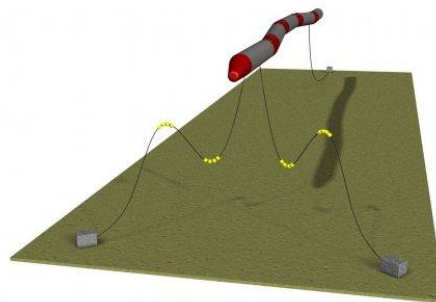
Figure 1.4: The Pelamis
(Pelamis Wave Power n.d.)

around the joints. This motion is resisted by hydraulic rams that pump high-pressure oil through hydraulic motors via smoothing accumulators. These hydraulic motors drive electrical generators to produce electricity. A Pelamis wave farm can be formed by a number of devices connected to an sea bed cable through an umbilical cable which the power from all the joints is fed down.

1.4 Outline of the Thesis

Chapter 2 is the theory chapter where the ocean waves theory, mass-spring-damper dynamics, hydrodynamics and maximum power capture are presented. It also contains a electrical analogue to the mechnical mass-spring-damper system.

The modeling chapter 3 presents the equations needed to model a axisymmetric point absorber WEC. The excitation force acting on the buoy is also presented with different methods for calculation. An open-loop analysis roundups the chapter.

The model is built in the graphical simulation tool Simulink and this is the subject for chapter 4 together with different control strategies. To be able to simulate on the model, a control strategy must be included, and I have included PID control and Model Predictive Control as strategies to be able to capture maximum power with Phase Latching.

At last there is a chapter were further work and some concluding remarks are given.

Chapter 2

Theory

This chapter will give an introduction to many fields, like ocean surface waves, the loop dynamics of a mass-spring-damper-system, the dynamics of a floating body in heave. Also the hydrodynamics of offshore devices and the energy absorption by oscillating bodies are presented. The findings in this chapter are the fundaments of chapter 3.

2.1 Ocean surface waves

An understanding of the ocean wave environment is fundamental to be able to explore the possibilities there is in capturing wave energy. This chapter will present many of the fundamental characteristics of the ocean environment.

2.1.1 Creation of waves

Waves are formed due to wind energy. In fact, the waves are a condensed form of solar energy. Wind sweeps over the earth's surface because of the unevenly heating from the sun. Heated air expands and its pressure drops which in turn forces the warm air to rise. When the warm air rises, cold air is dragged under to fill the empty space, and a circulation of air is begun. This is what we call wind.

Since land heats quicker than water this leads to greater thermal pressure on the coastlines. This is therefore these areas are likely to be more exposed to rougher wind conditions than inland areas.

The rotation of the earth does also have an effect on the wind formation. The Coriollis effect causes the longitudinal flow of air to be disrupted as winds are deflected to the right of their course in the northern hemisphere and to the left in the southern hemisphere. Cells of circulating air is formed,

three in each hemisphere. By definition, Norway lays on the border between the Polar cell and the Ferrel cell, but is regarded to be a part of the Westerlies (known as Vestavindsbeltet in Norwegian), (Meteorologisk institutt n.d.)

When wind travels over ocean water, it creates ripples on the surface. These are often called capillaries, and as they grow the wind gets better friction on the surface. This turns the ripples into chops after a period time, and the chops transform into small waves when the wind increase. Large waves and swell may then be formed if the wind continues to blow and increases in strength. The size of the waves are determined by wind
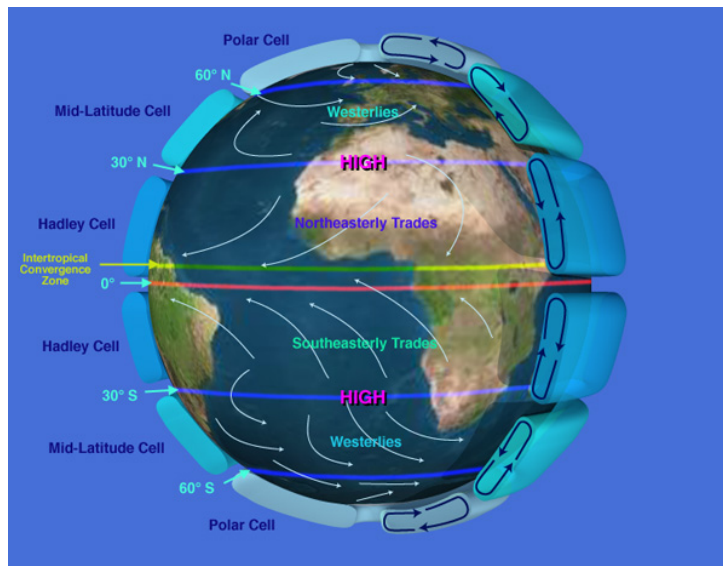
Figure 2.1: The global circulation of air.
(NASA 2008)

velocity, wind duration and fetch(the horizontal distance the waves are able to develope on), and together these determine the total amount of energy stored in the wave.

2.1.2 Wave equations

The fundamental wave equation describes all wave behavior a is commonly known as

$$\frac{\partial^2 u}{\partial t} = c^2 \nabla^2 u \tag{2.1}$$

where ∇^2 is the Laplacian and c is the velocity of the wave's propagation. The Laplacian is three-dimensional, but as the simulations is only performed

in two dimension equation 2.1 reduces to the two-dimensional wave equation

$$\frac{\partial^2 u}{\partial t} = c^2 \left(\frac{\partial^2 u}{\partial x^2} + \frac{\partial^2 u}{\partial y^2} \right) (Kreyzig\ 1999, p.583).$$

(2.2)

If $c = v_p$ is the "phase velocity" the wave propagates with in positive and negative x-direction, then v_p is obtained from the dispersion relation and is given after a long series of equations, which are beyond the scope of this thesis to reproduce, as

$$v_p \equiv \frac{\omega}{k} = \frac{g}{\omega} \tanh(kh) = \left\{ \frac{g}{k} \tanh(kh) \right\}^{1/2} (Falnes\ 2005, p.70).$$

(2.3)

where $k = 2\pi/\lambda$ is the wave number, h is the depth of the water and g is the gravitational force.
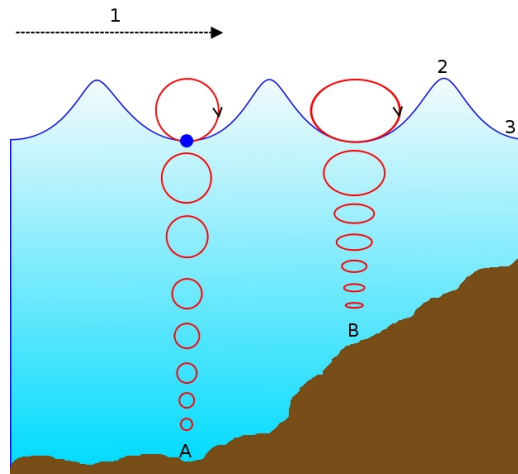
Figure 2.2: The water moves in orbits which diminish with increasing depth. (Wikimedia 2007)

The water particles in a wave move in circular orbits, with a radius near the surface almost equal to the amplitude of the wave. This circular motion displaces water, which means that the wave transmits energy as it travels. As seen from figure 2.2 the orbits diminish with respect to increasing depth, and the radii of the orbits can be considered to be negligible at a depth of $\lambda/2$. Here 1 is the direction of propagation of the wave, 2 is the crest, and 3 is the through of the wave. The following equations gives the horizontal, $\hat{v}_x$,

and vertical, $\hat{v}_z$, fluid velocities, respectively.

$$
\begin{aligned}
\hat{v}_x = \frac{\partial \hat{\phi}}{\partial x} &= g\frac{k}{\omega}e(kz)(\hat{\eta}_f - \hat{\eta}_b) \\
&= \omega\frac{\cosh(kz + kh)}{\sinh(kh)}(\hat{\eta}_f - \hat{\eta}_b) \quad (2.4)
\end{aligned}
$$

$$
\begin{aligned}
\hat{v}_z = \frac{\partial \hat{\phi}}{\partial z} &= g\frac{ik}{\omega}e'(kz)(\hat{\eta}_f + \hat{\eta}_b) \\
&= i\omega\frac{\sinh(kz + kh)}{\sinh(kh)}(\hat{\eta}_f + \hat{\eta}_b), \quad (2.5)
\end{aligned}
$$

where

$$
e'(kz) = \frac{de(kz)}{d(kz)} = \frac{\sinh(kz + kh)}{\cosh(kh)} = e(kz)\tanh(kz + kh). \quad (2.6)
$$

z is the depth below the surface. Here, k is the wave number, h is the water depth, $\hat{\eta} = \hat{\eta}_f + \hat{\eta}_b$ is the complex amplitude of the wave (Falnes 2005, p. 70-71), and $\hat{\phi}$ is the complex amplitude of the velocity potential(Falnes 2005, p. 64).

2.1.3 Wave Transport of Energy

Potential energy is related by the elevation of water from the wave through the wave crest (Falnes 2005, p. 75).

$$
E_p = mgh = \frac{1}{2}kh^2 \quad [J] \quad (2.7)
$$

where m is the mass, g is the gravitation force and h is the potential height and k is the restoring force coefficient applied if an object is moved a distance h from its equilibrium(Tipler and Mosca 2004, p. 434). The time-averaged potential energy per unit (horizontal) in a harmonic wave is given by the

$$
E_p(x, y) = (\rho g/4)|\hat{\eta}(x, y)|^2 \quad [J/m^2] \quad (2.8)
$$

where $\hat{\eta}$ is the amplitude of the wave (Falnes 2005, p. 76). For a progressive, plane harmonic wave we have

$$
E_p(x, y) = (\rho g/4)|A|^2 \quad [J/m^2] \quad (2.9)
$$

Kinetic energy is given by

$$
E_k = \frac{1}{2}mv^2 \quad [J] \quad (2.10)
$$

where m is the mass and v is the speed of the object (Tipler and Mosca 2004, p. 434). By integrating the average kinetic energy per unit volume from $z = -\infty$ to $z = 0$ (Falnes 2005, p.76, eq. 4.124) the average kinetic energy per unit (horizontal) area:

$$E_k = \frac{\rho}{2}\omega^2|A|^2 \int_{-\infty}^{0} e^{2kz}dz = \frac{\rho}{2}\frac{\omega^2}{2k}|A|^2 \tag{2.11}$$

Using $\omega^2 = gk$ we obtain

$$E_k(x,y) = (\rho g/4)|A|^2 \quad [J/m^2]. \tag{2.12}$$

As can be expected from the equipartition theorem, (Tipler and Mosca 2004, p. 544), the kinetic energy in a wave is equal to the potential energy in the wave. The total energy in a wave is accordingly a summation of kinetic and potential energy in the wave, and thus the time-average stored energy per unit (horizontal) area for a progressive, plane, harmonic wave is (Falnes 2005, p. 77)

$$E_{tot} = (\rho g/2)|A|^2 \quad [J/m^2]. \tag{2.13}$$

The energy per unit crest length is found by multiplying equation 2.13 by the wavelength of the wave.

$$E_L = (\rho g/2)|A|^2 \lambda \tag{2.14}$$

The power per unit crest length is found based on the knowledge that all the energy in the wave is transmitted completely with each successive wave, and diving equation 2.14 by the period of the wave gives

$$P = \frac{\rho g|A|^2 \lambda}{2T} \quad [W/m] \tag{2.15}$$

In deep water the wavelength equals $\lambda = gT^2/(2\pi)$ (Falnes 2005, p. 72), so the power per unit crest on deep water is

$$P = \frac{\rho g^2 H^2 T}{4\pi} \quad [W/m]. \tag{2.16}$$

2.2   Loop dynamics of a Mass-Spring-Damper System

This section is dedicated to the mass-spring-damper(MSD) system, and it's properties, since the point absorber WEC can be regarded as a MSD system. A stability analysis for the MSD system is also presented.
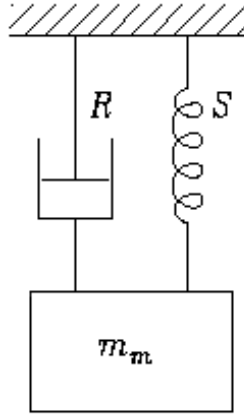
Figure 2.3: A schematic of a Mass-Spring-Damper System
Freely after (Falnes 2005, p. 202)

The MSD system is a secondary oscillatory system described by Egeland and Gravdahl (2002, p. 42) and (Falnes 2005, p. 4). The MSD system can be given as a differential equation

$$m_m\ddot{x} + R\dot{x} + Sx = F_{res}. \tag{2.17}$$

where m_m is the mass, R is the viscous friction coefficient (damping constant) and S is the spring constant. The MSD system is shown in 2.3. A state-space model representation for the MSD system is given by (Egeland and Gravdahl 2002, p. 10 f.f.)

$$\begin{aligned}
\dot{\boldsymbol{x}}(t) &= \boldsymbol{A}\boldsymbol{x}(t) + \boldsymbol{B}u(t) \\
y(t) &= \boldsymbol{C}\boldsymbol{x}(t) + Du(t).
\end{aligned} \tag{2.18}$$

The transfer function for this system is found by using the Laplace transform

$$\mathcal{L}\{\dot{\boldsymbol{x}}(t)\} = s\boldsymbol{x}(s) \tag{2.19}$$

on the model 2.18 to get

$$\begin{aligned}
s\boldsymbol{x}(s) &= \boldsymbol{A}\boldsymbol{x}(s) + \boldsymbol{B}u(s), \\
y(s) &= \boldsymbol{C}\boldsymbol{x}(s) + \boldsymbol{D}u(s).
\end{aligned} \tag{2.20}$$

By eliminating $\boldsymbol{x}(s)$ the transfer function $H(s)$ between the input $u(s)$ and the output $y(s)$ is found

$$\begin{aligned}
y(s) &= \left[C(sI - A)^{-1}B + D\right]u(s) \\
&= H(s)u(s)
\end{aligned} \tag{2.21}$$

$$\frac{y}{u}(s) \;\; = \;\; H(s) \tag{2.22}$$

The equation

$$y(s) = H(s)u(s) \tag{2.23}$$

is called the plant (Egeland and Gravdahl 2002, p. 14).
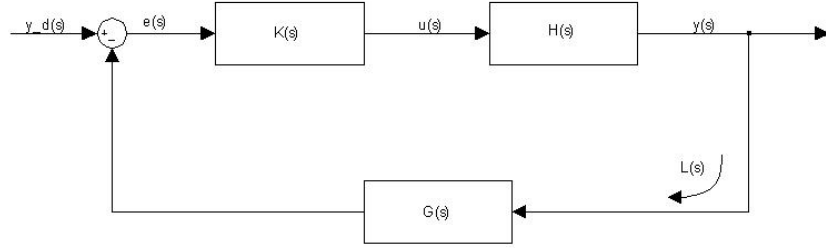
Figure 2.4: The transfer function of the loop

The transfer function of the loop given in figure 2.4 where H(s) is the transfer function of the plant, G(s) is the transfer function of the feedback controller, and K(s) is the compensation feedback controller. $u(s)$ and $y(s)$ is respectively the input and the output to the plant in equation 2.23, $y_d(s)$ is the desired setpoint, and $e(s)$ is the error between the desired setpoint and the output of the plant. Thus we have the following relations for the input $u(s)$ and the error $e(s)$

$$u(s) = K(s)e(s) \tag{2.24}$$

$$\begin{aligned} e(s) &= y_d(s) - G(s)y(s) \\ &= y_d(s) - G(s)H(s)K(s)e(s) \end{aligned} \tag{2.25}$$

where the loop transfer function is given by

$$L(s) = G(s)H(s)K(s). \tag{2.26}$$

The transfer function from the desired setpoint to the error is

$$S(s) := \frac{e}{y_d}(s) = \frac{1}{1 + L(s)}. \tag{2.27}$$

and is called the *sensitivity function S(s)*. The stability of the closed loop is found by studying the sensitivity function $S(s)$, which should have the poles with negative real parts.

The *cloosed-loop transfer function $T(s)$* is the one from the closed-loop input y_d to $y(s)$

$$T(s) := \frac{y}{y_d}(s) = \frac{K(s)H(s)}{1+L(s)} = \frac{1}{G(s)}\frac{L(s)}{1+L(s)} \approx \begin{cases} \frac{1}{Gs} & |L(s)| \gg 1 \\ K(s)H(s) & |L(s)| \ll 1 \end{cases}.$$
(2.28)

The *complementary sensitivity function* is obtained when the unity feedback is used, that is when $G(s) = 1$ and is given by

$$T(s) = \frac{L(s)}{1+L(s)} = 1 - S(s).$$
(2.29)

2.2.1   Performance of a Closed-Loop System

Obtaining a Bode Diagram for the loop transfer function $L(j\omega)$ is a useful way to apply frequency response techniques to specify the performance of a control system (Egeland and Gravdahl 2002, p.43 f.).

The magnitude of the sensitivity function $S(j\omega)$ will satisfy the approximations

$$|S(j\omega)| = \left| \frac{1}{1+L(s)} \right| = \begin{cases} |L(j\omega)^{-1}| & |L(j\omega)| \gg 1 \\ 1 & |L(j\omega)| \ll 1 \end{cases},$$
(2.30)

while the magnitude of the closed-loop transfer function T(s) is

$$|T(j\omega)| = \left| \frac{L(s)}{1+L(s)} \right| = \begin{cases} |L(j\omega)^{-1}| & |L(j\omega)| \gg 1 \\ 1 & |L(j\omega)| \ll 1 \end{cases}.$$
(2.31)

To reduce the effects of disturbances of the system the sensitivity $|S(j\omega)|$ should be small for low frequencies, while the complementary sensitivity function $|T(j\omega)|$ on the contrary should be small for high frequencies to reduce the influence of measurement noise and unmodeled dynamics. Thus, $|L(j\omega)|$ should be large for low frequencies and small for large frequencies. The reader is referred to (Egeland and Gravdahl 2002, p.43, figure 2.2) for a figure showing the requirements of the loop transfer function $L(j\omega)$.

The *Bode-Nyquist criterion* is used to state whether a system is stable or not. For a rational loop transfer function $L(s)$ with no poles in right half-plane, then the system is stable if

$$|L(j\omega_{180})| < \text{ and } \angle L(j\omega_c) - 180°$$
(2.32)

where ω_{180} is $\angle L(j\omega_{180}) = 180°$ and ω_c is the cross-over frequency ($|L(j\omega_c)|$). The stability margins are the margin $\triangle K$ and the phase margin ϕ and are,

in terms of $L(j\omega)$

$$\triangle K \quad := \quad \frac{1}{|L(j\omega_{180})|} > 1 \tag{2.33}$$

$$\phi \quad := \quad 180° + \angle L(j\omega_c) > 0° \tag{2.34}$$

2.3   Dynamics of a Floating Buoy in heave

In this section the dynamics of a sphere of radius a restricted to oscillation in the heave mode will be presented.

The hydrostatic buoyancy force F_b originates from the static-pressure term $-\rho g \eta$ because of the body's wet surface experiences varying hydrostatic pressure as a result of its oscillation. It is assumed linear conditions such that the hydrostatic buoyancy force F_b is proportional to the excursion η from its equilibrium position. It is common to express the buoyancy force as

$$F_b = -S_b \eta \tag{2.35}$$

where S_b is the *buoyancy stiffness* (Falnes 2005, p. 182 f.). A sphere with radius a and mass $m_m = \rho 2\pi a^3/3$ is in equilibrium when semi-submerged. When the sphere is displaced upward a distance η the volume of displaced water is $\pi(2a^3 - 3a^2\eta + \eta^3)/3$. The restoring force is hence $F_b = \rho g\pi(a^2\eta - \eta^3)/3$. Then the buoyancy stiffness is

$$S_b = \pi\rho g a^2(1 - \eta^2/3a^2) \tag{2.36}$$

if the displacement is less than the radius of the sphere, $|\eta| < a$. For small excursions, $|\eta| \ll a$, the buoyancy stiffness is

$$S_b \approx \pi\rho g a^2. \tag{2.37}$$

Clearly, that is ρg multiplied with the water plane area and then the buoyancy stiffness is independent of η.

In general, the buoyancy stiffness for a floating body with small excursions is

$$S_b \quad = \quad \rho g S_w \tag{2.38}$$

where S_w is the water plane area of the body. For a cylinder of radius a the water plane area is independent of the heave position, and $S_w = \pi a^2$. It is assumed that the buoy is cylindrical for now on.

2.4 The Hydrodynamics of Offshore Devices

Hydrodynamics is a sub-disipline of fluid dynamics and means the study of liquid in motion. The foundational axioms of fluid dynamics are the conservation laws(Egeland and Gravdahl 2002, p. 401), specifically, conservation of mass, conservation of linear momentum (Newtons Second Law), and conservation of energy. Since the key concept when modelling WECs is performance, and it is the overall goal to keep the performance on an acceptable level some hydrodynamical approximations is common to make(Cruz 2007, p. 52 f.f.).

The wave field in water of depth h may be characterized by an amplitude a, a wave number k ($\lambda = 2\pi/k$) and the radian frequency ω. These are related by a radiation function $G(a, k, \omega) = 0$. For the incident wave the surface elevation is

$$\eta(x, y, t) = a\cos(kx\cos\beta + ky\sin\beta - \omega t) \tag{2.39}$$

The mean power for the incident wave is

$$P_w = \frac{1}{2}\rho g a^2 c_g \tag{2.40}$$

where c_g is the group velocity for the waves.

The capture width is a measurement of the device's ability to absorb power

$$\mathcal{L}(\omega, \beta) = \frac{P}{P_w} \tag{2.41}$$

where P is the mean power absorbed by the device.

For an single thight-moored semi-submerged axisymmetric sphere the following holds

$$m_m \ddot{X} = F_f(t) + F_{ext}(X, \dot{X}, t) \tag{2.42}$$

where $F_f(t)$ are the wave induced forces and $F_{ext}(X, \dot{X}, t)$ are the externally applied forces. The wave induces forces are separated into

$$F_f(t) = F_s(t) + F_r(t) + F_h(t) \tag{2.43}$$

where F_s is the exciting force the buoy experiences if it is fixated in it's mean position, while $F_r(t)$ is the radiation force the body experience in addition of it's own oscillatory motion in otherwise calm water. At last, $F_h(t)$ is the hydrostatic buoyancy force applied on the body caused by the body's wet surface.

2.5   Wave-energy absorption by Oscillating Bodies

An oscillating body in water produces waves. The size of the wave produced depends on the size of the body and of which amplitude the body oscillates. A small body oscillating with bigger amplitude than the amplitude of the incident wave may be utilised for the purpose of wave-energy conversion.

In order to absorb wave energy Falnes (2005, p. 196 f.f.) states that it is necessary to displace water in an oscillatory manner and with correct phase, in other words, the energy has to be removed from the waves in energy conversion purpose. This means that there has to be a cancellation or reduction of the the incident waves passing by or reflected by the energy-converting device. One way to obtain this is if the oscillating device generates waves which interfere destructively with the waves, that is, the device has to generate waves which are in counterphase to the incident waves.

Figure 2.5 illustrates the oscillating bodies' ability to generate waves. Curve a shows a harmonic incident wave. The curves b and c illustrates the properties of evenly spaced, small floating bodies in oscillation on otherwise calm water. The first illustrates symmetric wave generation by heave, while the second illustrates antisymmetric wave generation. Curve d is a super-postion of the above three waves, and illustrates complete absorption of the incident wave.
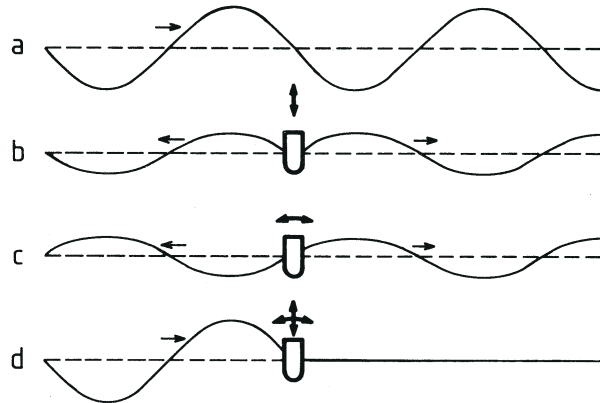

Figure 2.5: Illustration of oscillating bodies ability to generate waves.
(Falnes 2005, p. 197)

In the case of a symmetrical body in vertical oscillations (heave), only 50% absorption is possible if there is only symmetrical radiated waves. For

a point absorber the maximum possible energy to be absorbed by a heaving axisymmetric body equals the incident wave front of width equal to the wavelength divided by 2π. This may be refered as the absorption width. For maximum energy to be absorbed, optimum oscillations by the WEC is necessary, and in case of a sinusoidal incident wave there excists an optimum phase and an optimum amplitude for the oscillations. The optimum amplitude is proportional to the amplitude of the incident wave.

With one mode of oscillations, vertical heave, the resulting wave corresponds to the superposition of curve a and b from figure 2.5. The phase of the oscillator has to be correct corresponding to the incident wave, because the crest of the waves radiated toward the right must conicide with the throughs of the incident wave. The aim is therefore for the oscillator to have resonance with the incident wave.

The wave radiated toward the left and the resulting wave transmitted toward the right both have an amplitude equal to half of the incident wave. This means that 25% of the incident wave is reflected toward the left and 25% of it is transmitted toward the right, because wave energy is proportional to the square of the wave amplitude. The remaining 50% is absorbed by the WEC, and this is as previously mentioned the theoretical maximum of absorption for a point absorber.

An incident wave produces an excitation force F_e, and the body responds to this force with an oscillation of velocity $\dot{\eta}$. The total force acting on the system is $F_t = F_e - F_r$, where F_r is the radiation force resulting when the buoy oscillates. The power absorbed by the ball is obtained by multiplying the total force by the velocity of the ball, $P_t(t) = F_t(t) \cdot \dot{\eta}(t)$. The time-average power is $P_t = \frac{1}{\Delta t} \int F_t \dot{\eta} \, dt$.

In order to absorb wave power a certain fraction of the excitation power P_e acting on the ocsillating body is necessarily returned as radiated power because of interference between the radiated wave and the incident wave. Methods to overcome the radiation problem will be discussed in chapter 4.2.

2.6 Maximum power capture

Some sort of control is necessary to be able to obtain maximum power from the WEC, or else it would not be possible to get the buoy to respond with correct phase and amplitude in correspondence with the incident wave.

Budal's latching-controlled buoy principle is one of the most recognized principle for approximated optimum energy conversion, and the principle was first proposed by Budal and J. Falnes (1980) and is also presented in (Falnes 2005, p. 206 f.f.). This method will be investigated below.

As was stated in the previous section, energy has to be removed from the waves in order to absorb energy, and in order to obtain maximum energy form the waves it is necessary to have optimum oscillation of the wave-energy converter. The optimum oscillation consists both of an optimum phase and an optimum amplitude. For oscillation in heave, the resulting wave corresponds to the superposition of the incident wave propagated in x-direction and the wave radiated from the buoy. For optimum oscillation the amplitude of the radiated wave have to be exactly half of the amplitude of the incident wave. Thus it is required that the amplitude of the vertical oscillation of the WEC have proper value. The wave radiated to the left and the resulting wave transmitted to the right both have amplitude equal to the half of the amplitude of the incident wave.

2.6.1   Phase control by latching

For a one-mode oscillating system, when the wave frequency is the same as the natural frequency of the oscillating system, the oscillating system happens to have the optimum condition if it is in resonance with the wave. Bandwidths that are close enough to the resonance gives approximately optimum, and the sufficient bandwidth size is greater for WECs of large extension than for those of smaller extension. It is therefore a design quest to make as small as possible WECs with satisfactory bandwidth.

Some of the energy may be returned back to the sea in small fractions of each oscillations while aiming to obtain maximum converted energy. Then it is possible to profit from that the rest of the cycle. This is called "reactive control", and it is required to utilize a reversible energy-converting machinery with very low conversion losses, e.g a high-efficiency hydraulic machinery or a linear generator. Additionally, a computer with appropriate software and with input signals from sensors measuring the wave and/or the WEC's oscillatory motion, is required.

Figure 2.6.1 shows another, approximative, method for optimum control which is possible if the wave periods are longer than the WEC's natural period. This is called "latching phase control", where a clamping mechanism stops the motion of the WEC at the instant of extreme excursion, that is, when the velocity becomes zero. The buoy is then released after a certain time before the next extremum of the wave exciting force appears. Curve a: Elevation of the water surface caused by the incident wave (at the position of the buoy). This would also represent the vertical position of a body with negligible mass. For a body of diameter very small compared with the wavelength, curve a also represents the wave's heave force on the body. Curve b: Vertical displacement of a heaving body whose mass is so large that
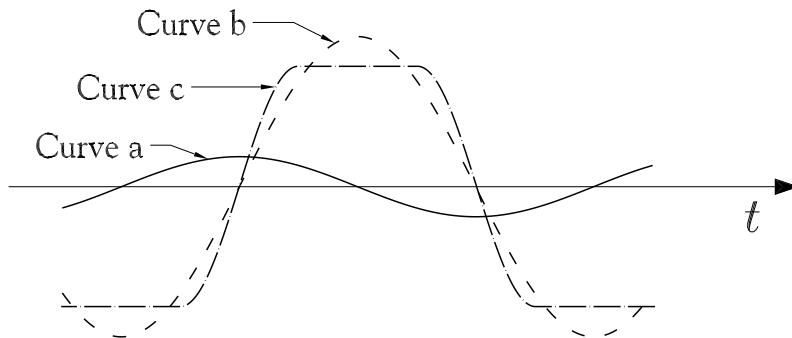
Figure 2.6: Resonance and phase control. The curves indicates wave elevation and vertical displacement of (different versions of) a heaving body as functions of time.

(Falnes 2005, p. 207)

its natural period is equal to the wave period (resonance). Curve *c*: Vertical displacement of a body with smaller mass, and hence a shorter natural period. Phase control is then obtained by keeping the body in a fixed vertical position during certain time intervals.

2.7 Power take-off systems

In order to convert the wave-energy to electrical energy, there has to be a power take-off system connected between the buoy and the grid.

2.7.1 Electrical analogue

The mechanical system consisting of a mass, spring and a damper that was given in figure 2.3 has an electric circuit analogue shown in figure 2.7. This electric circuit is well-known as the RLC-circuit and consists of an inductance m, a capacitance $1/S$ and an electric resistance R connected in series. The driving voltage is analogous to the resultant force F, the position x is analogous to the electric charge on the capacitance and the velocity $\dot{x}$ is analogous to the electric current. The reason for using this electric analogue is to explain and calculate the effects that generator damping control has on a WEC system. By applying Krichhoff's law on the circuit in figure 2.7, the equation 2.17 is obtained. The energy is stored in the capacitance as electric energy (analogous to potential energy) and in the inductance as magnetic

energy (analogous to kinetic energy). When $x(t) = 0$, the potential energy is zero while the magnetic energy is zero when $\dot{x} = 0$. At resonance the potential and the kinetic energy are equal, and the energy is swinging back and forth between the two energy stores, twice every period of the system's forced oscillation.
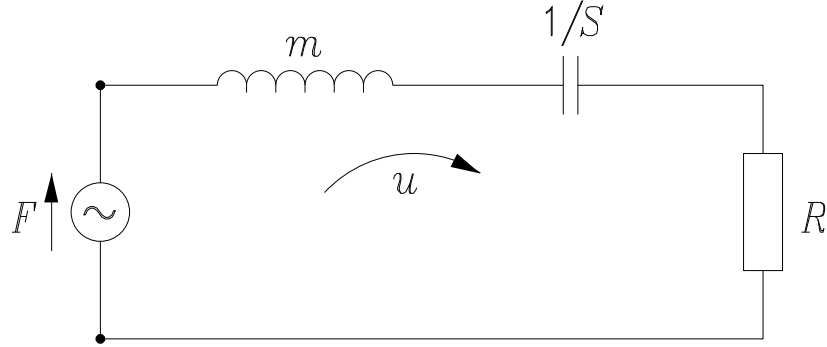

Figure 2.7: Electric analogue of the mass-spring-damper system.
(Falnes 2005, p. 9)

Introducing mechanical impedance Z for for equation 2.17 with sinusoidally varying quantities represented by their complex amplitudes inserting

$$F(t) = \frac{\hat{F}}{2}e^{i\omega t} + \frac{\hat{F}}{2}e^{-i\omega t} \tag{2.44}$$

$$x(t) = \frac{\hat{x}}{2}e^{i\omega t} + \frac{\hat{x}}{2}e^{-i\omega t} \tag{2.45}$$

into 2.17

$$\left[\hat{F} - \left(R + i\omega m + \frac{S}{i\omega}\hat{x}\right)\right]e^{i\omega t} + \left[\hat{F}^* - \left(R - i\omega m - \frac{S}{i\omega}\hat{x}^*\right)\right]e^{-i\omega t}. \tag{2.46}$$

The complex "mechanical impedance" is

$$Z = i\omega m + R + S/(i\omega) = R + i(\omega m - S/\omega), \tag{2.47}$$

and that leads up to

$$(\hat{F} - Z\hat{x})e^{i\omega t}) + (\hat{F}^* - Z^*\hat{x}^*)e^{i\omega t}) = 0. \tag{2.48}$$

An electric impedance is the ratio between complex amplitudes of voltage and current, and analogously, the mechanical impedance is the ratio between the complex force amplitude and the complex velocity amplitude. Mechanical impedance has the SI unit dimension

$$[Z] = \frac{N}{m/s} = \frac{kg}{s} \tag{2.49}$$

2.7.2 Hydraulic power take-off

A hydraulic power take-off system is where the motion of the floating body is converted into flow of a liquid, often oil, at high pressure by mean of hydraulic rams. A the other end of the hydraulic circuit there is a hydraulic motor that drives an electric generator.

2.7.3 Linear generator

Linear generators with large diameter coils and a large number of turns in order to increase the voltage at the terminals are suitable for use in wave energy conversion, because they are robust without rotating parts.

Chapter 3

Modeling

This chapter will present the ideas and equations needed to be able to create model for simulations in the graphical Matlab tool Simulink which will be presented in chapter 4.

3.1 System choises and limitations

The choice of buoy is a sphere-shaped point absorber, and the choice was made on the basis of the paper (Hals 2008, p.1 f.f.) by Ph.D Jørgen Hals from the Centre of Ships and Ocean Structures and the work of professor emeritus Johannes Falnes of the department of physics, both at Norwegian University og Science and Technology.

As stated in chapter 2, to make a good wave absorber a body will need to have the ability to generate relatively large waves when exposed to oscillations. Hals (2008) states that a ball has these properties when it intersects the surface, and by make a limitation on the diametre to be small compared to the wavelength on the incoming waves, such a ball may have the potential to be one of the most energy effective wave energy converters. The radius is chosen to be $a = 5m$, and with a mass m_b that gives an equlibrium when the ball is semi-submerged, $m = \frac{2\pi}{3}\rho a^3$. Figure 3.1 shows a skecth where the vertical sweep in the z-direction is called η [m], while the waves propagate in the x-direction. A machinery force between the ball and the bottom, is marked with the sign PTO[1].

This model will perform as a regulatory model and the following will be assumed in that matter:

- *Hydrodynamical exitation.* The ball's shell experience a dynamic pressure from the water because of the waves passing by, which gives rise
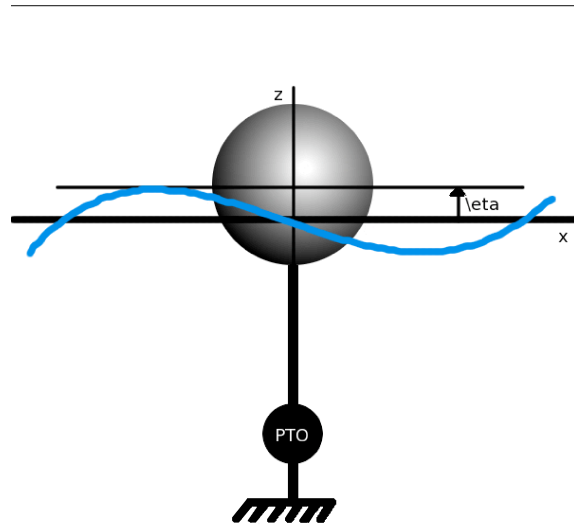
---

[1]Power Take-Off

Figure 3.1: An oscillating semi-submerged ball with radius 5m is used as an example of a point absorber

to a total force called *the exitational force F_e*. Only the vertical forces are considered.

- *Hydrodynamical radiation.* The motion of the buoy causes motions in the water, which in return act back on the buoy with a reaction force. This force is separated in a term propotional to the acceleration of the buoy, $A(\omega)\ddot{\eta}$ and one term which is proportional to the velocity of the buoy, $B(\omega)\dot{\eta}$. The proportionality constants are named *added mass(A)* and *radiant resistance (B)*.

- *Netto lifting force F_c.* Only the difference between the gravitational force and the lifting force is included in the equations, that is $F_c = m_b g - \rho V_S g \approx \rho g A_\omega(\eta)\eta = C\eta$. The area of the water plane A_ω is dependent on the position of the ball, but in this case it is set be constant.

- *Force of inertia $F = m_b\ddot{\eta}$.* This force is due to the change in velocity for the ball.

- *Force of machinery F_m.* This force is dependent of what type of machinery is chosen and how this is controlled. One assumption is to let the machinery be infinite rapid with infinite amount of force.

Linear hydrodynamic is used in the regulator model, that is, the hydro-dynamical forces increase linearly with the wave height and is not dependent of the position of the buoy. It is assumed that there are only deep water waves, it means that the depth $h > \lambda/3$, where λ is the wave length.

The power balance for the system in the frequency domain is $\{m_b + A(\omega)\}\ddot{\eta} = -B(\omega)\dot{\eta}(\omega) - C\eta(\omega) + F_e(\omega)$. Since multiplication in the frequency domain corresponds to convolution in the time domain, the first two terms on each side of the equation mark is convoluted in the time domain. By combining these terms, and separating $A(\infty) = lim_{\omega\to\infty}A(\omega)$ from the added mass the following equation is obtained

$$\dot{p}(t) = -A(\infty)\ddot{\eta}(t) - \int_0^\infty k(\tau)\eta(t-\tau)d\tau - C\eta(t) + F_m(t) + F_e(t) \quad (3.1)$$

where $p = m_b\dot{\eta}$ is the velocity of motion of the buoy, and $k(t)$ is a retardation function. The convolution term represents the radiated wave force, $F_r = \int_{-\infty}^t k(t-\tau)n(\tau)$. A convolution term is often not desired in a time domain equation. The convolution term is therefore usually approximated by a state space model, as in (Taghipour, T. Perez and T. Moan 2007):

$$\dot{\mathbf{z}}(t) = \mathbf{A}_r\mathbf{z}(t) + \mathbf{B}_r\dot{\eta}(t) \quad (3.2)$$
$$F_r = \mathbf{C}_r\mathbf{z}(t) \quad (3.3)$$

By choosing the velocity of motion and position as the state space variables the system may be written on state space form:

$$\dot{x} = \begin{bmatrix} 0 & \frac{-C_b}{1+m_{infty}/m_b} & \frac{-C_r}{1+m_{infty}/m_b} \\ 1/m_b & 0 & \mathbf{0} \\ \boldsymbol{B}_r/m_b & \mathbf{0} & \boldsymbol{A}_r \end{bmatrix} \boldsymbol{x}$$

$$+ \begin{bmatrix} \frac{1}{1+m_{infty}/m_b} \\ 0 \\ \mathbf{0} \end{bmatrix} F_m + \begin{bmatrix} \frac{1}{1+m_{infty}/m_b} \\ 0 \\ \mathbf{0} \end{bmatrix} F_e$$

$$\equiv \boldsymbol{A}_{ct}\boldsymbol{x} + \boldsymbol{B}_{u,ct}F_m + \boldsymbol{B}_{d,ct}$$
$$= \boldsymbol{A}_{ct}\boldsymbol{x} + \boldsymbol{B}_{u,ct}F_m + W \quad (3.4)$$

where it is the machinary force F_m that is subject to control. The system

matrices is found to be

$$
A_{ct} = \begin{bmatrix}
0 & -5.283e+005 & 231.3 & -6.843 & 101.8 & -20.75 \\
3.727e-006 & 0 & 0 & 0 & 0 & 0 \\
-0.001289 & 0 & -1.11 & 1.204 & -1.087 & 0.1938 \\
-3.812e-005 & 0 & -1.204 & -0.001028 & 0.02767 & -0.006427 \\
0.0005673 & 0 & 1.087 & 0.02767 & -2.149 & 1.217 \\
0.0001156 & 0 & 0.1938 & 0.006427 & -1.217 & -0.3189
\end{bmatrix}
\tag{3.5}
$$

$$
B_{u,ct} = B_{d,ct} = \begin{bmatrix}
0.6689 \\
0 \\
0 \\
0 \\
0 \\
0
\end{bmatrix}.
\tag{3.6}
$$

The eigenvalues of the system matrix is three complex conjugated pair, all of them in the right half-plane. This means that the system in it self is stable.

3.2 Excitation force - different methods

There are several methods to calculate the excitation force that act of the buoy, and the Froude-Krylov approximation and a state-space approximation are presented below.

3.2.1 Foude-Krylov approximations

For a fixed body, an incident wave results in a non-vanishing potential $\hat{\phi}$. According to (Falnes 2005, p. 122), the force on the body F_j is called the excitation force, and it has the generalised vector

$$
\boldsymbol{F}_e \equiv (F_{e,1}, F_{e,2}, \ldots, F_{e,6}) = (\vec{F}_3, \vec{M}_e)
\tag{3.7}
$$

where

$$
F_{e,j} = i\omega\rho \iint_S \left(\hat{\phi}_0 + \hat{\phi}_d \right) n_j \, dS.
\tag{3.8}
$$

$\hat{\phi}_0$ represents the undisturbed incident wave and $\hat{\phi}_d$ represents the diffracted wave that is induced when the former wave does not satisfy the homogenous boundary condition on the fixed surface S. If the diffraction term $\hat{\phi}_d$ is neglected in equation 3.7, the resulting force is termed the Froude-Krylov force. This is considered as a reasonable approximation to the excitation

force if the extension of the immersed body is very small compared with the wavelength. The generalized vector for the excitation force is (Falnes 2005, p. 160)

$$\hat{\boldsymbol{F}}_{e,p} = \hat{\boldsymbol{F}}_{FK,p} + \hat{\vec{F}}_{d,p} \tag{3.9}$$

We will now consider the excitation forces on a heaving axisymmetric body, where the z axis is the axis of symmetry (Falnes 2005, p. 166 f.). In this case φ_3 is symmetric, whereas n_1 and n_2 are antisymmetric, and it follows that the radiation impedance $Z_{13} = 0$ and $Z_{23} = 0$ which leads to $m_{13} = m_{23} = 0$. For $j = q = 1, 2, 3$ and approximation for $F_{e,j}$ gives

$$\hat{F}_{e,q} \approx \rho g \hat{\eta}_0 S_\omega \delta_{q3} + \rho V \left(1 + \mu_{qq}\right) \hat{a}_{0q} \tag{3.10}$$

where

$$\mu_{jj} = m_{jj}/\rho V \tag{3.11}$$

is the non-dimensionalised added-mass coefficient.

From Eqs. 3.9 and 3.10 the excitation force in heave mode ($j = q = 3$) is

$$\hat{F}_{e,3} = \hat{F}_{FK,3} + \hat{F}_{d,3} = \left[\rho g S_\omega + (\rho V + m_{33})\frac{\hat{a}_{03}}{A}\right] A. \tag{3.12}$$

For a small floating body with $z \approx 0$ on deep water this simplifies to

$$\hat{F}_{e,3} = \left[\rho g S_\omega - \omega^2 \rho V (1 + \mu_{33})\right] A. \tag{3.13}$$

Thus we have an approxmation for the diffraction force

$$\hat{F}_{d,3} \approx \omega^2 \rho V (1 + \mu_{33}) \tag{3.14}$$

and the approximation is linear in k on deep water where $\omega^2 = gk$.

3.2.2 State-space estimation

The excitation force F_e as well as the incident wave is independent of the motion of the buoy (Yu and J. Falnes 1996, p. 271). But it is practical to use the measured incident wave as input in ocean engineering because it is more general.

A state-space model may be used to approximate the excitation force $y_f(t) = F_e(t)$ where the incident wave is the input $u(t) = \eta(0, t) = a(t)$. $\eta(0, t)$ is the wave elevation at the origin. The excitation force $F(i\omega)$ is expressed in the frequency domain as (Ibid., p. 268)

$$\begin{aligned}
F_e(i\omega) &= H_f(i\omega)\eta(0, i\omega) \\
&= H_f(i\omega)A(\omega) \\
&= H_f(\omega)e^{i\theta_f \omega}A(\omega).
\end{aligned}$$

$H_f(\omega)$ and $\theta_f(\omega)$ are the amplitude and phase of the excitation force coefficient, respectively. taking the inverse Fourier transform of equation 3.15 gives the excitation force in the time domain

$$f_e(t) = \int_{-\infty}^{\infty} h_f(t-\tau)\eta(0,\tau)d\tau = \int_{-\infty}^{\infty} h_f(t-\tau)a(\tau)d\tau \qquad (3.15)$$

where $\eta(x,t)$ is the incident wave elevation in the time domain, and $a(t)$ is as given above. $h_f(t)$ is the time domain excitation force coefficient for heave. $h_f(t)$ is not casual (Ibid., p. 271), in the means that the chosen input is not the cause of the output. What is really causing the heave excitation force may be a distant storm. Then the generated wave may hit the body and exert a wave force before any wave has reached the reference point $x = 0$ (chosen conveniently).

A state-space description for the excitation force when $h_f(t)$ is non-casual is

$$\dot{\boldsymbol{X}}_f(t) = \boldsymbol{A}_f\boldsymbol{X}_f(t) + \boldsymbol{B}_f u(t) \text{ with } \boldsymbol{X}_f(0) = 0 \qquad (3.16)$$

and

$$y_f(t) = \boldsymbol{C}_f\boldsymbol{X}(t+t_c) \approx \int_{\infty}^{\infty} h_f(t-\tau)\eta(0,\tau)d\tau \qquad (3.17)$$

where $\boldsymbol{X}_f$, $u(t) = \eta(0,t)$ and $y_f(t) \approx f_e(t)$ are the state vector, the input variable and the output variable of the linear subsystem, respectively. Determination of the system matrices $\boldsymbol{A}_f$, $\boldsymbol{B}_f$ and $\boldsymbol{C}_f$ is done by minimizing the a target function, that is

$$Q = \sum_{k=1}^{m} G(t_k)\left[h_{fc}(t_k) - \boldsymbol{C}_f e^{\boldsymbol{A}_t t_k}\boldsymbol{B}_f\right]^2 \qquad (3.18)$$

where $h_{fc}(t) = h_f(t - t_c)$ is the causalised impulse response function corresponding to $h_f(t)$.

3.3 Open loop stability analysis

The eigenvalues of the system matrix is three complex conjugated pair, all of them in the right half-plane. This means that the system in it self is stable.
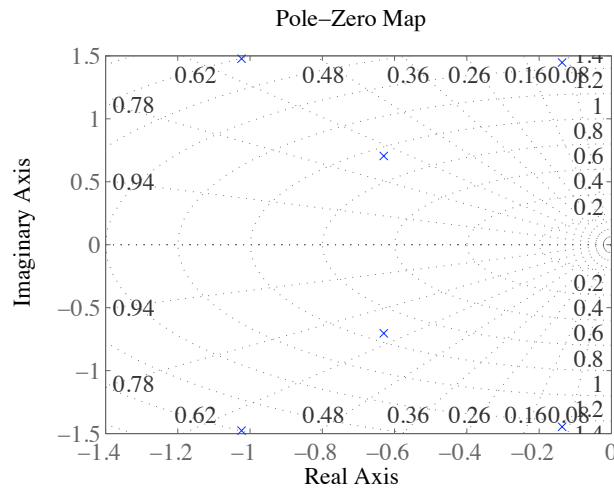
Figure 3.2: The eigenvalues of the system
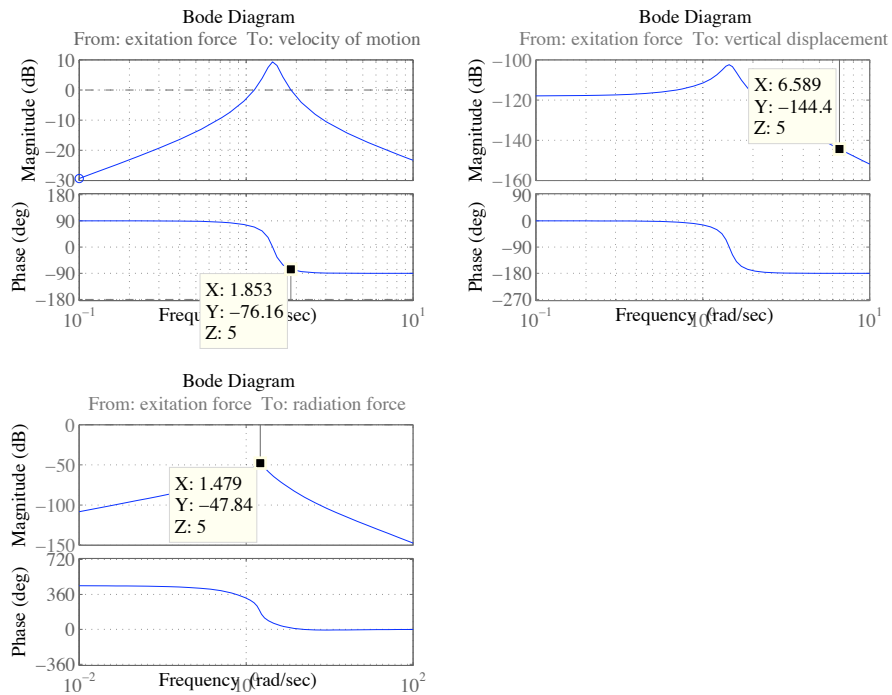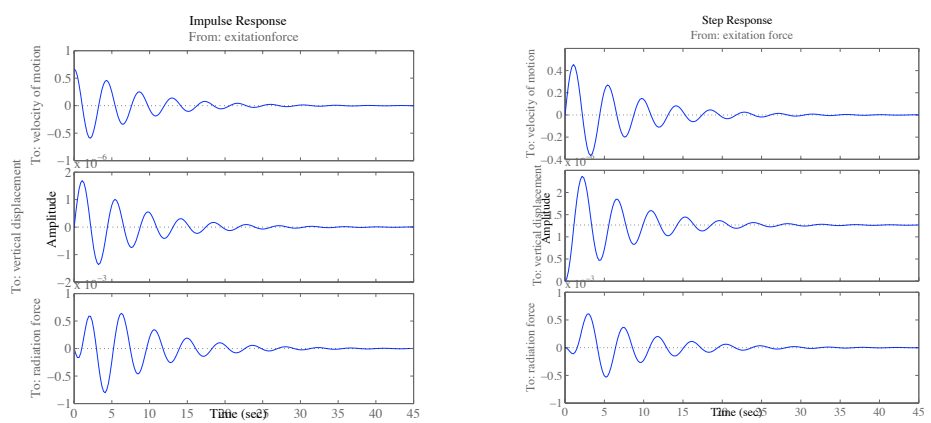

Figure 3.3: The Bode plot for exiation force input

(a) The Impulse response from the exitation force to the various outputs

(b) The step response resulting from applying a step signal

Figure 3.4: Impulse and step response

Chapter 4

Simulation

This chapter shows the simulation of the buoy performed in the Simulink, which is a graphic modeling tool on the Matlab platform. Simulink is a powerful tool which makes it possible to use non-linearities such as saturation and delays without cumbersome mathematical deductions first. Secondly it allows the user to implement all of the equation into a single workspace. It is also easily possible to import and export data to and from the simulations.

4.1 The Wave Energy Converter system

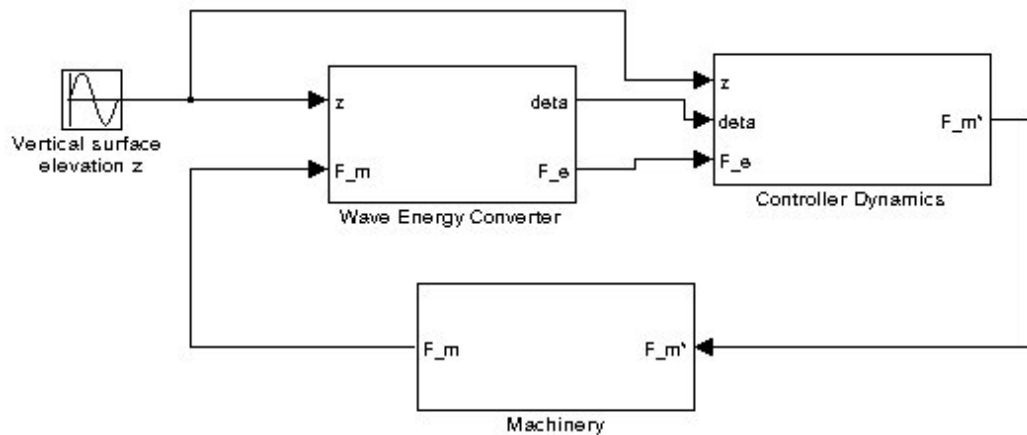A high-level look at the organization of the complete wave energy system is shown in figure 4.1.

Figure 4.1: A schematic of the top-level WEC system

The system is separated in three different subsystems, like a physical separation. The dynamics for the Wave Energy Converter has the inputs

vertical surface elevation z and the machinery force F_m, while the outputs are the elevation velocity $deta = \dot{\eta}$ for the buoy and the excitation force F_e. The Wave Energy Converter is further divided in the subsystems given in figures 4.3(a) and 4.3(b), respectively the excitation force block and the buoy dynamics block. Figure 4.2 shows an overview over the unrestrained system,
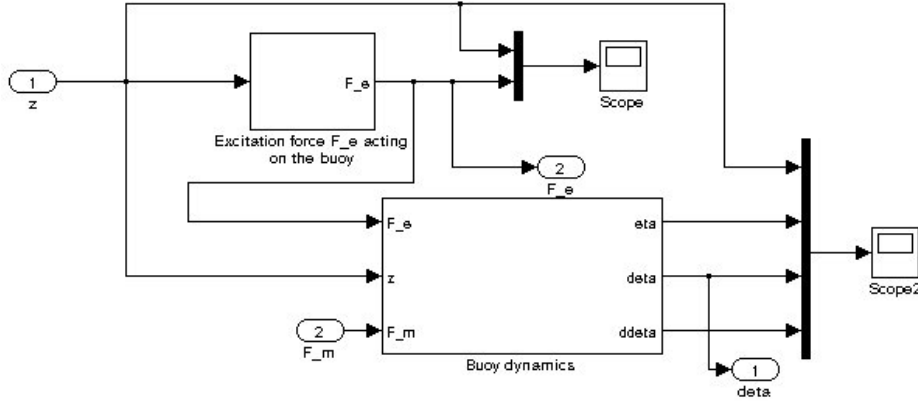

Figure 4.2: The unrestrained system

while figure 4.3 shows the subsystems of the unrestrained system. Figure 4.3(a) and figure 4.3(b) shows how the wave excitation force respectively the buoy dynamics are build up. These are based on the findings in chapter 3. The incident wave to *Excitation force F_e acting on the body* block has the water surface elevation z as input, and the excitation force as output F_e. It consists of the method for calculating the excitation force as was given in chapter 3. The *Buoy dynamics* block has the excitation force F_e and the machinery force F_m, while the outputs are elevation $eta = \eta$, velocity $deta = \dot{\eta}$ and acceleration $ddeta = \ddot{\eta}$ of the buoy. It is possible to include the water surface elevation as an input to the Buoy dynamics block to include limitations that results from violating the freeboard and draft of the buoy like it is showed in 4.4.

Using the content in table 4.1 the free response of the WEC for a couple of periods is shown in figure **??**, when a incident wave is present.

4.2 Natural frequency

For a single degree of freedom(SDOF) oscillator, a system in which the motion can be described by a single coordinate, the natural frequency depends on two system properties; mass m and hydrostatic stiffness S_h. The circular
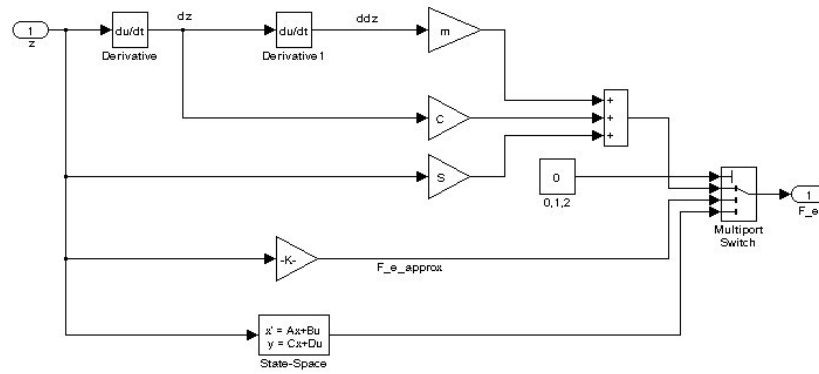
(a) Excitation force F_e acting on the buoy
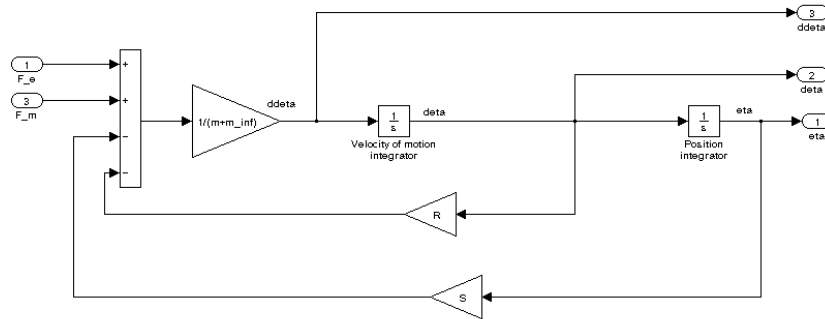
(b) The buoy dynamics

Figure 4.3: The Simulink system

Table 4.1: Name, value, dimension and description of the different unit used in simulation (In courtesy of Jørgen Hals)

| Name	Value	SI Dimension	Description
g:	9.8100	m/s^2	The acceleration of gravity
rho:	1025	kg/m^3	Water density
h:	100	m	Water depth
domega:	0.0631	rad/s	Frequency step
omega:	[200x1]	rad/s	Angular frequency vector
k:	[200x1]	m^{-1}	Wave number vector
a:	5	m	Sphere radius
m:	2.6834e+05	kg	Mass of sphere
Awp:	78.5398	m^2	Spheres water plane surface area
V:	261.7994	m^3	Submerged volume of sphere
S:	7.8974e+05	N/m	Hydrostatic stiffness of sphere at initial position
m_inf:	1.3283e+05	kg	Added mass at infinite frequency
omega_0:	2.4383	rad/s	Eigen angular frequency for the column
T_0:	2.5768	s	Eigen period for the column
H_F:	[200x1]	N/m	Excitation force coefficient
R_r:	[200x1]	kg/s	Radiation resistant
m_r:	[200x1]	kg	Added mass
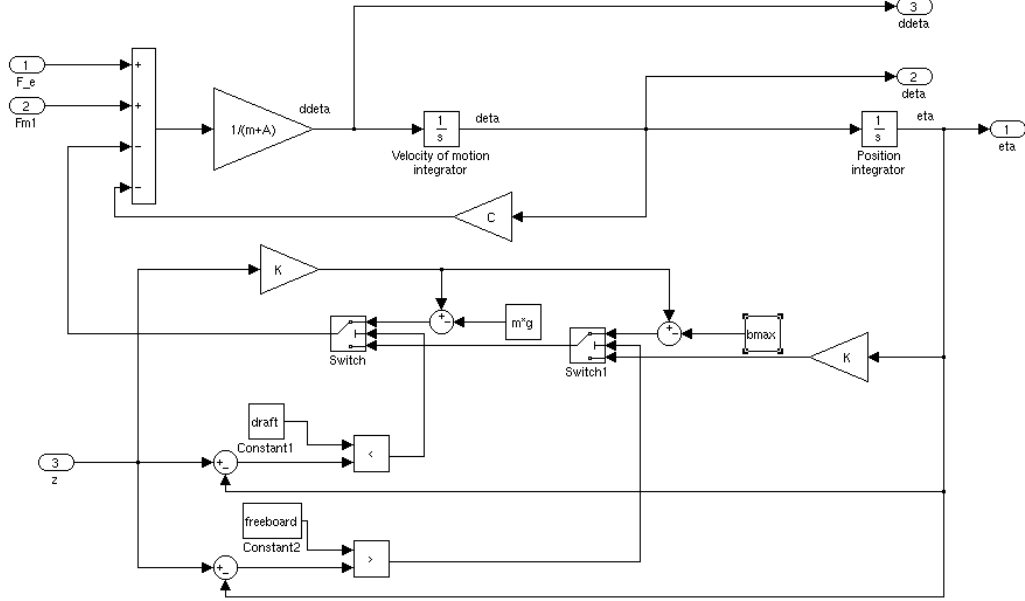
Figure 4.4: The buoy dynamics if limitations on freeboard and draft is included

natural frequency, ω_n, can be found using the following equation:

$$\omega_n^2 = \frac{S_h}{m_b + m_\infty}, \tag{4.1}$$

where S is the hydrostatic stiffness of the sphere, m is the mass, and ω_n is the circular natural frequency (radians per second)

From the circular frequency, the natural frequency, f_n, can be found by simply dividing ω_n by 2π. Without first finding the circular natural frequency, the natural frequency can be found directly using:

$$f_n = \frac{1}{2\pi} \sqrt{\frac{S_h}{m_b + m_\infty}}, \tag{4.2}$$

where f_n is natural frequency in hertz (1/seconds), S is the hydrostatic stiffness of the sphere (N/m), and m is the mass (kg) When we insert the proper values in 4.2, $m_b = 2.6834e + 05$, $m_\infty = 1.3283e + 05$, and $S = 7.8974e + 05$, we find the circular natural frequency to be $\omega_n = 1.4031$ and the natural frequency to be $f_n = 0.2233$. Using this in the simulation, the response of the WEC will hopefully be close to resonance. A Bode plot for the WEC would show the natural frequency.

4.3   Proportional-Integral-Derivative control

Proportional-Integral-Derivative controllers (PID controllers) are widely used in industrial control systems. It is a feedback loop controller with three separate parameters, and it attempts to correct the error between the desired set-point and a measured variable.

The PID algorithm performed on the error involves the three parameters: The Proportional value determines the reaction to the current error, the Integral value determines the reaction based on the sum of recent errors, and the Derivative value determines the reaction based on the rate at which the error has been changing.

To achieve the best response possible of the system tuning of the three parameters is required, although optimal control or stability is not guaranteed with use of the PID controller. But it is often possible to obtain both small stationary deviation and high band width.

The transfer function for an ideal PID controller is

$$h_r(s) = K_p \left(1 + \frac{1}{T_i s + T_d s} \right) \approx K_p \frac{(1 + T_i s)(1 + T_d s)}{T_i s} \tag{4.3}$$

where the approximation is valid if $T_d \ll T_i$. A process controlled by an ideal PID controller is shown in figure 4.5.
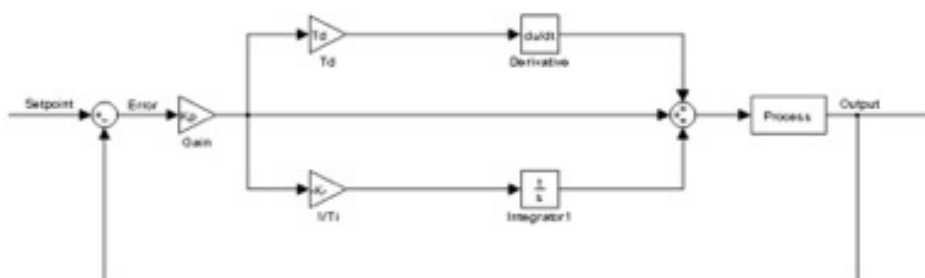

Figure 4.5: A process controlled by an ideal PID Controller

4.4   Model-based predictive control

In contrary to PID control, Model-based predictive control (MPC) and the extremum seeking method handles constraints. With MPC it is possible to constrain both the inputs and the measurements. This is an advantage because operation closer to constraints frequently leads to more profitable operation (Maciejowski 2002, p. 1).

4.4.1   MPC in the loop

The advantages with use of MPC are many and the computer hardware is so fast now that it is possible to use MPC on a wide variety of problems. In the case with a wave energy converter, it will be possible to predict the future behavior of the incident wave, and use this to latch and unlatch the buoy at the right time in a manner that don't violate the constraints on the measurements and states.

4.4.2   The control hierarchy

Maciejowski (2002, p. 28) gives an overview over a control hierarchy where predictive control is involved. The control hierarchy may be transferred to the wave energy converter, shown in figure 4.6. In contrary to the figure represented on (Maciejowski 2002, p.27) the local loop controllers layer are omitted, because as with flight or spacecraft control, there is no scope for individual loops in the wave energy converter as holding each set-point requires coordinated action by several actuators.

4.4.3   The 'receding' horizon idea

MPC is based on iterative, finite horizon optimization of a plant model. At time t a numerical minimization algorithm performs a cost minimization control strategy for a future time horizon; [t, t+T] that is relatively short in respect to the production time horizon. An idea called *the 'receding' horizon*[1] is discussed in (Maciejowski 2002, p. 7 f.f.). The idea is that a plant at current time t has output $y(k)$, and that there is a *set-point trajectory $s(k)$* which the output should follow and a *reference trajectory $r(k)$* starting from $y(k)$ that will bring the output $y(k)$ back on the set-point trajectory on an ideally

---

[1]The name is given because the prediction horizon remains the same length at each iteration, like the Earth's horizon recedes when moving towards is, the distance is alway the same.
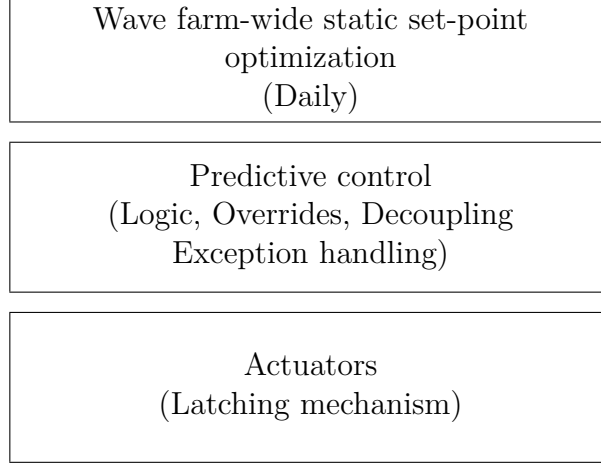
Wave farm-wide static set-point optimization (Daily)

Predictive control (Logic, Overrides, Decoupling Exception handling)

Actuators (Latching mechanism)

Figure 4.6: Use of predictive control

basis. The current error may origin from a disturbance and is given by

$$\epsilon(k) = s(k) - y(k). \tag{4.4}$$

The reference trajectory is chosen such that the error i steps later, if the output followed it exactly, would be

$$
\begin{aligned}
\epsilon(k+i) &= e^{iT_s/t_{ref}}\epsilon(k) \\
&= \lambda^i\epsilon(k),
\end{aligned}
\tag{4.5}
$$

where T_s is the sampling interval and $\lambda = e^{T_s/T_{ref}}$ is the exponentially approach from the current output value to the set-point trajectory. The reference trajectory is then defined to be

$$
\begin{aligned}
r(k+i|k) &= s(k+i) - \epsilon(k+i) \\
&= s(k+i) - e^{-T_s/T_{ref}}\epsilon(k)
\end{aligned}
\tag{4.6}
$$

where it is shown that the reference trajectory depends on the conditions at time k.

An internal model is used to predict the behavior of the plant and the goal is to find the input which promises the best predicted behavior. The internal model is predicted over a future prediction horizon H_p, starting at the current time, and depends on the assumed input trajectory $\hat{u}(l+i|k)$ $(i = 0, 1, \ldots, H_p - 1)$ which is to be applied over the prediction horizon.

The assumed input $\hat{u}(k+i|k)$ at time $k+i$ will probably differ from the actual input $u(k+i)$ at the same time since $\hat{u}(k+i|k)$ depends on the

information available at current time k and thus is a predicted input. Using
the current output $y(k)$ when deciding the input value $u(k)$ implies that the
internal model is strictly proper, that is, it must only depend on past inputs
$u(k-1), u(k-2), \ldots$, but not on the current input $u(k)$.

There are several ways to choose how the input trajectory is computed for
the reference trajectory to reach the required value, *the coincidence point*, at
the end of the prediction horizon, at time $k+H_p$. Some may require the least
amount of energy spent, while the simplest way is to assume that the input
remains constant over the prediction horizon and thus satisfies the equation
$-\hat{y}(k+H_p|k) = r(k+H_p|k)$, an equation which have a unique solution.

When the choice of input trajectory method is taken and a future input
trajectory has been computed, only the first element of this trajectory is
applied as the input to the plant, that is $u(k) = \hat{u}(k|k)$. Then the new output
$y(k+1)$ is measured, the reference trajectory $r(k+i|k+1)$ $(i = 2, 3, \ldots)$ is
defined, the predictions over the horizon $k+1+i$, with $i = 1, 2, \ldots, H_p$ are
run, and the input trajectory $\hat{u}(k+1+i|k+1)$ with $i = 0, 1, \ldots, H_p - 1$ is
chosen; all of this is done one sampling interval later to be able to find the
next input to the plant: $u(k+1) = \hat{u}(k+1|k+1)$. This cycle goes on as
long as the plant is controlled by this predictive control method.

4.4.4   Formulation of a Qudratic Problem for MPC

A standard QP formulation is on the form (Hovd n.d.)

$$
\begin{aligned}
\underset{v}{min} \quad & 0.5v^T H v + c^T v \\
\text{s.t. constr} \quad & Lv \le v
\end{aligned}
\tag{4.7}
$$

To get an MPC problem into the QP problem formulation these steps are
taken.

$$
\begin{aligned}
f(x, u) = f(\chi_{dev}, \chi_v, v) &= (x_0 - x_{ref,0})^T Q(x_0 + x_{ref,0}) + \\
& \quad (\chi_{dev} + \chi_v)^T \hat{Q}(\chi_{dev} + \chi_v) + v^T \hat{P} v \\
&= (x_0 - x_{ref,0})^T Q(x_0 + x_{ref,0}) + (\chi_{dev})^T \hat{Q}(\chi_{dev}) \\
& \quad + \chi_{dev}^T \hat{Q}\chi_v + \chi_v^T \hat{Q}\chi_{dev} + \chi_v^T \hat{Q}\chi_v + v^T \hat{P} v
\end{aligned}
\tag{4.8}
$$

The first two expressions which is independent of the free variable v and
therefore unnecessary to use in the minimization problem may be removed,
and then inserting $\chi_v = \hat{B}v$ gives

$$
\begin{aligned}
f(\chi_{dev}, \chi_v, v) &= 2\chi_{dev}^T \hat{Q}\chi_v + \chi_v^T \hat{Q}\chi_v + v^T \hat{P} v \\
&= 2\chi_{dev}^T \hat{Q}\hat{B}v + (\hat{B}v)^T \hat{Q}\hat{B}v + v^T \hat{P} v \\
&= 2\chi_{dev}^T \hat{Q}\hat{B}v + v^T \hat{B}^T \hat{Q}\hat{B}v + v^T \hat{P} v \\
&= v^T(\hat{B}^T \hat{Q}\hat{B} + \hat{P})v + 2\chi_{dev}^T \hat{Q}\hat{B}v
\end{aligned}
\tag{4.9}
$$

Then the QP formulation is obtained if the following is chosen

$$\begin{aligned} H &= \hat{B}^T \hat{Q} \hat{B} + \hat{P} \\ c^T &= \chi_{dev}^T \hat{Q} \hat{B} \end{aligned} \qquad (4.10)$$

Chapter 5

Conclusion

This chapter will make a survey of work that could be done to the control problem on posterior thesis, and the findings in the previous chapters.

5.1 Further work

The most urgent work that should be done in a further work is to make a complete simulation model that contains all parts needed for optimum energy absorption.

As we rarely encounter an ideal ocean conditions, optimum control is not a real option in order to maximize the energy harvest. Therefore, control actions must be taken with real-world criteria in minds. The electric circuit analogue from chapter 2 will be used to explain some the limitations that have effect on the energy absorption.

5.2 Results and Conclusion

In the thesis several concepts of Wave energy converters, and there is modeled a WEC of point absorber type. In the simulation chapter both PID control and Model Predictive Control is presented as solutions to the optimization problem. Model Predictive Control, although it is more complex, is probably the best control strategy with use on a WEC point absorber, because it can "foresee" the incoming waves some time into the future. Model Predictive Control can also guarantee stability.

Bibliography

Budal, K. and Falnes, J.: 1985, Bølgjeenergiforskinga ved NTH. Historisk oversyn 1973-85, *Technical report*, Norwegian University of Science and Technology.

Budal, K. and J. Falnes: 1980, Interacting point absorbers with controlled motion in power from sea waves.

Cruz, J. (ed.): 2007, *Ocean Wave Energy: Current Status and Future Perspectives*, Springer.

Egeland, O. and Gravdahl, J. T.: 2002, *Modeling and Simulation for Automatic Control*, Marine Cybernetics.

Falnes, J.: 2005, *Ocean waves and oxcillating systems*, 1st paperback edn, Cambridge University Press.

Hals, J.: 2008, Matematisk model for ei halvt nedsøkkt kule i hiv, *Technical report*, Centre of Ships and Ocean Structures.

Hovd, M.: n.d., Model-based predictive control, urlhttp://... Last visited on April 1, 2009. The paper is available from the link 'Utdrag fra kompendium' on top of the page.
URL: *www.itk.ntnu.no/ansatte/Hovd_Morten/VGProsreg/Litteratur .html*

Kreyzig, E.: 1999, *Advanced Enginerring Mathematics*, 8th edn, John Wiley & Sons, Inc.

Maciejowski, J. M.: 2002, *Predictive Control - with Constraints*, Pearson/Prentice Hall.

Meteorologisk institutt: n.d., Klimaet i norge. Last visited on March 19, 2009.
URL: *met.no/?module=Articles;action=Article.publicShow;ID=806*

NASA: 2008, The global circulation of air. Last visited on March 30, 2009.
  URL: *http://sealevel.jpl.nasa.gov/overview/climate-climate.html*

Pelamis Wave Power: n.d., Pelamis. Last visited on March 30, 2009.
  URL: *http://www.pelamiswave.com/gallerydiagram.php*

Renewable Energy Journal: 2007, The oscillating water column. Last visited
  on March 30, 2009.
  URL: *http://montaraventures.com/energy/2007/04/13/mechanical-ocean-energy-conversion-part-ii*

Taghipour, R., T. Perez and T. Moan: 2007, Hybrid frequency-time domain
  models for dynamic response analysis of marine structures, *Ocean Engineering, Volume 35, Issue 7, May 2008, Pages 685-705* .

Tipler, P. A. and Mosca, G.: 2004, *Physics for Scientists and Engineers*, 5th
  edn, W. H. Freeman and Company.

U.S. Department of Energy: n.d., The archimedes waves swing. Last visited
  on March 30, 2009.
  URL: *http://www1.eere.energy.gov/windandhydro/hydrokinetic/images %5Ctechnologies%5C4073f9a7-9500-43c9-9235-7dabd9ff3c09.JPG*

Wave Dragon: n.d., Wave dragon. Last visited on March 30, 2009.
  URL: *http://www.wavedragon.net/index.php?option=com_docman&task= cat_view&gid=15&Itemid=28*

Wikimedia: 2007, Orbital circulation of water particles. Last visited on
  March 30, 2009.
  URL: *http://commons.wikimedia.org/wiki/File:Wave_motion-i18n.svg*

Wu, M. and T. Moan: 1996, Linear and nonlinear hydroelastic analysis of
  high-speed vessels, *Journal of Ship Research, Volume 40, Pages 149-163*
  .

Yu, Z. and J. Falnes: 1996, State-space modelling of a vertical sylinder in
  heave.